Chinese Chemical Letters 33 (2022) 1609–1612

Contents lists available at ScienceDirect

Chinese Chemical Letters

journal homepage: www.elsevier.com/locate/cclet

A multisite-binding fluorescent probe for simultaneous monitoring of mitochondrial homocysteine, cysteine and glutathione in live cells and zebrafish

Huimin Jiang, Guoxing Yin, Yabing Gan, Ting Yu, Youyu Zhang, Haitao Li, Peng Yin*

Key Laboratory of Chemical Biology and Traditional Chinese Medicine Research (Ministry of Education), College of Chemistry and Chemical Engineering, Hunan Normal University, Changsha 410081, China

ARTICLE INFO

Article history:
Received 25 May 2021
Revised 7 September 2021
Accepted 8 September 2021
Available online 15 September 2021

Keywords:
Fluorescent probe
Multiple sites
Biothiols
Mitochondrial-targeted
Homocysteine
Imaging

ABSTRACT

Homocysteine (Hcy), cysteine (Cys) and glutathione (GSH) play crucial roles in redox homeostasis during mitochondria functions. Simultaneous differentiation and visualization of mitochondrial biothiols dynamics are significant for understanding cell metabolism and their related diseases. Herein, a multisite-binding fluorescent probe (MCP) was developed for simultaneous sensing of mitochondrial Cys, GSH and Hcy from three fluorescence channels for the first time. This novel probe exhibited rapid fluorescence turn-on, good water-solubility, high selectivity and large spectral separation for discriminating Cys, GSH and Hcy with 131-, 96-, 748-fold fluorescence increasement at 471, 520, 567 nm through different excitation wavelengths, respectively. Importantly, this probe was successfully applied to simultaneous monitoring of mitochondrial Cys, GSH, and Hcy in live cells and zebrafish from three fluorescence channels, promoting the understanding of the functions of Hcy, Cys and GSH.

Biothiols, such as cysteine (Cys), glutathione (GSH) and homocysteine (Hcy), are involved in a variety of physiological and pathological processes in complex biological environments [1–3]. Mitochondria as dynamic organelle are the central factory to produce ATP, reactive species, as well as exhibits biological roles in antioxidant activities [4,5]. Recent studies have revealed that mitochondria dysfunction is the root cause of many diseases, such as Alzheimer's disease, Parkinson's disease, due to the imbalanced redox homeostasis [6–9]. Nevertheless, Cys and GSH as the most abundant low molecular weight biothiols in biosystems (Cys: 30–200 μmol/L, GSH: 1–10 mmol/L in cells, respectively), play critical roles in maintaining cell functions [10–14]. On the other hand, Hcy is served as the substrate for the biosynthesis of Cys and GSH [15], and exhibits different physiological function from Cys/GSH, which could cause oxidative damage to cells [16]. Hence, it is of great value to simultaneously monitor mitochondrial Cys, GSH and Hcy dynamics for understanding their related physiological and pathological processes.

Recently, multi-signal fluorescent probes, which could simultaneously differentiate multiple biologically related species, have attracted great attention for tracing cellular dynamics, metabolism and biosynthesis events [2,17]. Pioneered by Guo's work [18], several coumarin-based fluorescent probes have been developed to simultaneously differentiate Cys/GSH/Hcy from different fluorescence channels with good sensitivity and good specificity [2,19–26]. Though a lot of fluorescent probes for visualizing Cys or GSH in mitochondria have been reported [27–34], monitoring mitochondrial Hcy is very rare. In our previous work, two fluorescent probes (named BCC and **1**, respectively, Scheme S2 in Supporting information) with multi-binding sites were developed for simultaneous sensing of Cys, Hcy, and GSH through different fluorescence channels [35,36]. However, the two fluorescent probes based on 2-(benzothiazol-2-yl)acetonitrile or cyanoacetate group showed moderate water solubility and poor organelle targeted property, which are not specific to monitor mitochondrial Cys/Hcy/GSH. Thus, fluorescent probes for simultaneously discriminating and visualizing mitochondrial Hcy, Cys and GSH could provide new perspectives for the research of mitochondrial functions, as well as promote molecular imaging in chemical biology.

Encouraging by our previous findings [35,36], we de-novo designed a novel fluorescent probe MCP with multi-binding sites for simultaneous visualization of mitochondrial Cys, GSH and Hcy (Scheme 1). Probe MCP was rationally designed with three potential reaction sites: *n*-butylthio group in the 4-position of the coumarin (site 1) for specific nucleophilic substitution between probe and Cys/GSH/Hcy; the α,β-unsaturated C=C bond (site 2)

* Corresponding author.
E-mail address: yinpeng@hunnu.edu.cn (P. Yin).

https://doi.org/10.1016/j.cclet.2021.09.036
1001-8417/

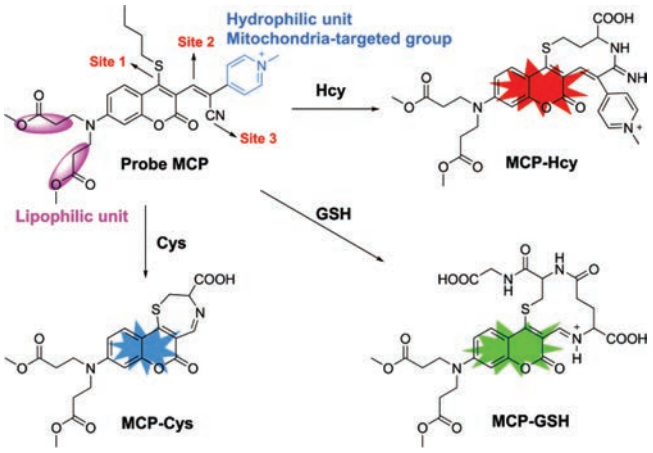

Scheme 1. The structure of probe MCP and the proposed mechanism for sensing of Cys, Hcy and GSH with probe MCP.

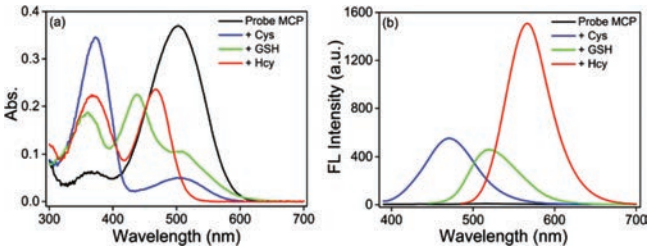

Fig. 1. (a) Absorption spectra of probe MCP (10 μmol/L) upon addition of 10 equiv. of Cys/GSH/Hcy (100 μmol/L) at 25 °C for 20 min. (b) The corresponding fluorescence spectra of probe MCP to 10 equiv. of Cys (λ_{ex} = 375 nm), GSH (λ_{ex} = 430 nm), and Hcy (λ_{ex} = 470 nm). Condition: DMSO-PBS (pH 7.4, 10 mmol/L, 2/8 (v/v)). Slit (nm): 2.5/2.5.

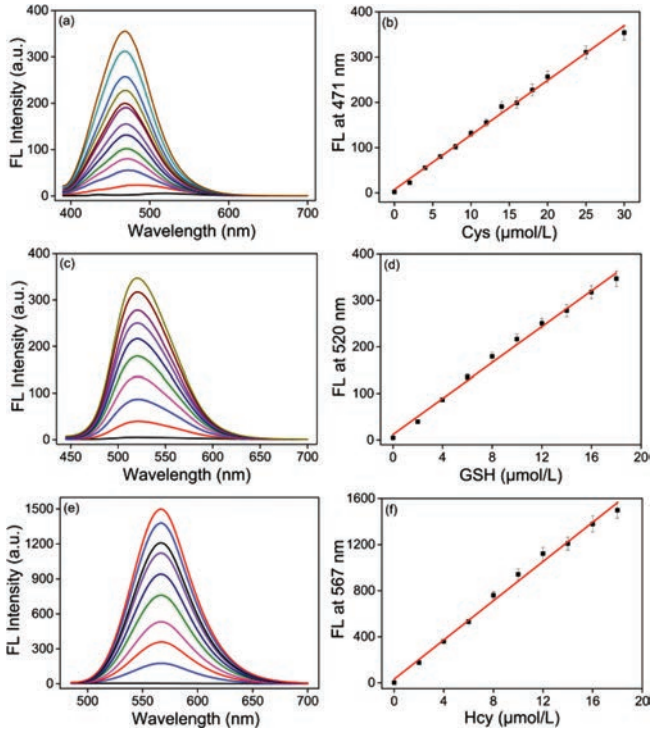

Fig. 2. Fluorescence intensity spectra of probe MCP (10 μmol/L) in the presence of (a) 0–30 μmol/L Cys excited at 375 nm, (c) 0–18 μmol/L GSH excited at 430 nm, (e) 0–18 μmol/L Hcy excited at 470 nm, respectively. The linear changes of the fluorescence intensities of probe MCP at 471, 520 and 567 nm and as a function of (b) Cys, (d) GSH and (f) Hcy concentrations, respectively. Condition: DMSO-PBS (pH 7.4, 10 mmol/L, 2/8 (v/v)) at 25 °C for 20 min. Slit (nm): 2.5/2.5.

for Michael-addition or amino addition, and the cyano group (site 3) for amino addition (a ten-membered ring fluorophore would be formed for Hcy). Thus, biothiols-induced substitution-cyclization cascade reactions would enable the simultaneous discrimination of Cys, GSH and Hcy *via* different emission channels. Furthermore, *N,N*-dimethyl propionate substituents in the coumarin fluorophore could enhance lipophilicity for plasma membrane penetrability [37]. The methylpyridinium unit was served as an excellent hydrophilic moiety as well as a mitochondria-targeted group [38]. Featured with these superiorities, this novel probe MCP exhibited rapid fluorescence turn-on for simultaneous differentiation of Cys ($\lambda_{ex}/\lambda_{em}$ = 375/471 nm), GSH ($\lambda_{ex}/\lambda_{em}$ = 430/520 nm) and Hcy ($\lambda_{ex}/\lambda_{em}$ = 470/567 nm) with large spectral separation, high selectivity, high sensitivity, and good water-solubility. Furthermore, this probe has been successfully applied to the simultaneous fluorescence imaging of mitochondrial Cys, GSH and Hcy in live cells and zebrafish, which will greatly promote the understanding of mitochondrial functions related to Cys/GSH/Hcy.

Initially, the synthesis of probe MCP was outlined in Scheme S1 (Supporting information). Detailed methodology and spectroscopic data were provided in the ESI (Scheme S1, Figs. S14–S16 in Supporting information), and its spectral properties for sensing of Cys, GSH and Hcy were carefully conducted *via* UV-vis spectroscopy and fluorescence spectroscopy in DMSO-PBS buffer (10 mmol/L, 2/8 (v/v)). As shown in Fig. 1, the maximum absorption spectra of probe MCP exhibited hypsochromic shift from 502 nm to 375, 430 and 470 nm upon addition of Cys, GSH and Hcy, respectively. Under different excitation wavelengths (λ_{ex} = 375 nm for Cys; λ_{ex} = 430 nm for GSH and λ_{ex} = 470 nm for Hcy), this probe showed significant fluorescence turn-on responses for discriminating Cys, GSH and Hcy along with 131-, 96-, 748-fold fluorescence increasement at 471, 520, 567 nm, respectively. As expected, this novel probe could selectively detect Cys, GSH and Hcy from distinct emission channels with large spectral separation ($\Delta\lambda \sim 50$ nm, Fig. 1), which were further supported by the time dependent UV-vis spectroscopy and fluorescence spectroscopy (Figs. S1–S7 in Supporting information). Probe MCP also displayed well-defined fluorescence profiles with good water solubility, moderate quantum yield ($\Phi_{MCP\text{-}Cys}$ = 3.4%, $\Phi_{MCP\text{-}GSH}$ = 6.4%, $\Phi_{MCP\text{-}Hcy}$ = 24.2% in DMSO-PBS buffer (2/8, v/v)) and favorable photostability for sensing Cys, GSH and Hcy (Fig. S8 in Supporting information). Thus, this probe can simultaneously discriminate Cys, GSH and Hcy from three emission channels under different excitation wavelengths.

Based on the proposed mechanisms of biothiols-induced substitution-cyclization cascade reactions (Scheme 1, Figs. S17–S19 in Supporting information), three fluorescent products with distinct photophysical properties could be obtained after the reaction between probe MCP with Cys, GSH and Hcy respectively. Thus, probe MCP is capable to detect Cys, GSH and Hcy from three emission channels (Scheme S3, Figs. S17−S19 in Supporting information). In order to clarify that probe MCP has the capability to detect Cys/Hcy/GSH specifically, the selectivity of probe MCP over other biologically related species including various amino acids, reactive sulfur species, reactive oxygen species and ions was further investigated. The fluorescence intensities of probe MCP were only significantly increased upon the addition of Cys/GSH/Hcy under the excitement at 375, 430 and 470 nm, respectively. No obvious fluorescence enhancement could be observed to a series of other biologically related species (Fig. S9 in Supporting information). We also found that probe MCP could selectively detect Cys, GSH and Hcy from the mixture of Cys/GSH/Hcy using specific fluorescence channels (Fig. S10 in Supporting information). Next, the fluores-

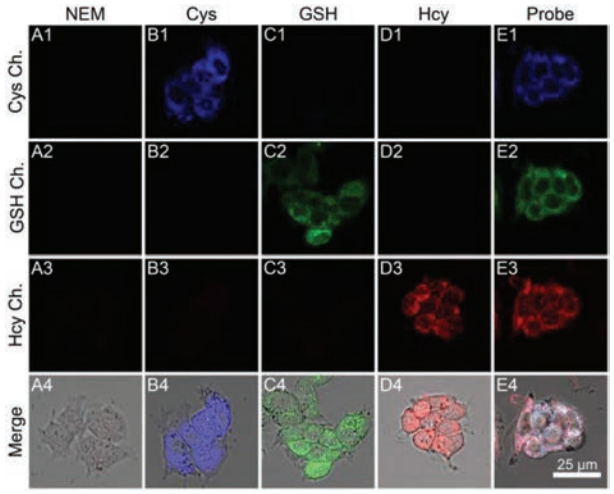

Fig. 3. Confocal fluorescence imaging of Cys, GSH, and Hcy in HepG2 cells. Cells were pretreated with NEM (0.1 mmol/L) for 30 min, then incubated with probe MCP (5 μmol/L) for 30 min (A1–A4). Cells were pretreated with NEM (0.1 mmol/L) for 30 min, subsequently incubated with Cys/GSH/Hcy (250 μmol/L, 30 min), respectively, and finally incubated with probe MCP (5 μmol/L) for 30 min (B1–D4). The cells were incubated with probe MCP (5 μmol/L) for 30 min, then imaged (E1–E4). λ_{ex} = 405 nm, λ_{em} = 420–475 nm for the blue channel; λ_{ex} = 458 nm, λ_{em} = 490–530 nm for the green channel; and λ_{ex} = 488 nm, λ_{em} = 550–620 nm for the red channel. Scale bar: 25 μm. For interpretation of the references to color in this figure legend, the reader is referred to the web version of this article.

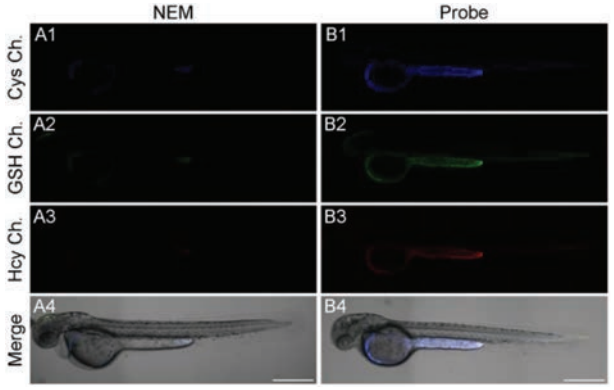

Fig. 4. Confocal fluorescence imaging of Cys, GSH, and Hcy in 2-day-old zebrafish. Zebrafish were pretreated with NEM (200 μmol/L) for 30 min and then incubated with probe MCP (5 μmol/L) for 60 min (A1–A4). Zebrafish were treated with probe MCP (5 μmol/L) for 60 min, then imaged (B1–B4). λ_{ex} = 405 nm, λ_{em} = 420 – 475 nm for the blue channel; λ_{ex} = 458 nm, λ_{em} = 490–530 nm for the green channel; and λ_{ex} = 488 nm, λ_{em} = 550–620 nm for the red channel. Scale bar: 0.5 mm. For interpretation of the references to color in this figure legend, the reader is referred to the web version of this article.

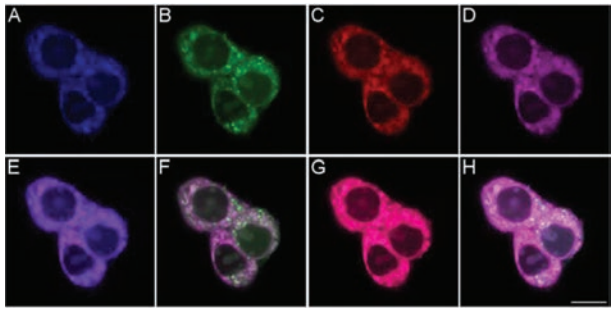

Fig. 5. Co-localization confocal fluorescence imaging of Cys, GSH and Hcy in HepG2 cells using probe MCP and Mito-Tracker Red. The cells were incubated with probe MCP (5 μmol/L) and Mito-Tracker Red (200 nmol/L) for 30 min at 37 °C, then imaged. (A) Blue channel for Cys, (B) green channel for GSH, (C) red channel for Hcy, (D) purple channel for Mito-Tracker Red. (E–G) Represent the overlay images of (A) and (D), (B) and (D), (C) and (D), respectively. (H) Represents the overlay images of (A–D). λ_{ex} = 405 nm, λ_{em} = 420–475 nm for the blue channel; λ_{ex} = 458 nm, λ_{em} = 490–530 nm for the green channel; λ_{ex} = 488 nm, λ_{em} = 550–590 nm for the red channel; λ_{ex} = 561 nm, λ_{em} = 600–650 nm for the purple channel. Scale bar: 10 μm. For interpretation of the references to color in this figure legend, the reader is referred to the web version of this article.

cence titration experiments of probe MCP toward Cys, GSH and Hcy were conducted respectively, and the fluorescence of probe MCP increased linearly with the concentrations of biothiols: 0−30 μmol/L for Cys, 0−18 μmol/L for GSH and Hcy, respectively (Fig. 2). Furthermore, the detection limits were calculated to be as low as 27.3, 45.9, 13.7 nmol/L for Cys, GSH and Hcy, respectively, indicating that probe MCP is highly sensitive for these thiols. Therefore, probe MCP has the potential to be applied to discriminate and fluorescence image of Cys, GSH, and Hcy from three emission channels *in vitro* and *in vivo*.

Subsequently, simultaneous visualization of endogenous Cys, GSH and Hcy in live cells and zebrafish using probe MCP was performed. Probe MCP showed minimum cytotoxicity to HepG2 cells within 24 h (Fig. S11 in Supporting information). When cells were pretreated with *N*-ethylmaleimide (NEM, a scavenger of biothiols) and successively incubated with Cys/GSH/Hcy and probe MCP respectively, specific and robust fluorescence was observed in blue, green and red fluorescence channels, respectively (Fig. 3 (A1−D4)). These results have well demonstrated that simultaneous fluorescence imaging of Hcy, Cys and GSH could be achieved with high selectivity. As expected, live cells were simultaneously exhibited bright blue, green and red fluorescence after incubation with probe MCP, indicating that it was realized for the simultaneous fluorescence imaging of endogenous Cys, GSH and Hcy (Fig. 3 (E1−E4)). Moreover, this probe could be also applied to visualize endogenous Cys, GSH and Hcy in zebrafish (Fig. 4). To further confirm that probe MCP has the capacity for targetable detection of biothiols in mitochondria, the live cells were co-incubated with probe MCP and Mito-Tracker Red. The strong fluorescence signals of probe MCP colocalized well with that of Mito-Tracker Red in mitochondria (Pearson's coefficient: blue for Cys: 0.85; green for GSH: 0.75, and red for Hcy 0.91 respectively), which demonstrated that probe MCP was well-stained in mitochondria for simultaneous sensing of Cys, GSH and Hcy (Fig. 5). These data suggested that probe MCP is powerful for fluorescence imaging of mitochondrial biothiols in living cells and zebrafish, possessing valuable applications for exploring the root causes of diseases related to mitochondrial thiols dynamics.

In summary, through the introduction of *N,N*-dimethyl propionate substituents and methylpyridinium moiety in coumarin fluorophore, a novel multisite-binding fluorescent probe MCP has rationally exploited for simultaneous discrimination of Cys, GSH and Hcy from different fluorescence channels with good water solubility, high selectivity, high sensitivity, and large spectral separation. Probe MCP was successfully applied to fluorescence image mitochondrial Cys, GSH, and Hcy simultaneously in live cells and zebrafish from three different emission channels for the first time. This novel fluorescent probe MCP possesses the potential for monitoring mitochondrial Cys, GSH and Hcy in biological system, and greatly promoting our understanding about mitochondrial functions related to biothiols dynamics.

Declaration of competing interest

The authors declare no competing financial interest.

Acknowledgments

This work was supported by the National Natural Science Foundation of China (Nos. 21877035 and 21977028) and Research Foundation of Education Bureau of Hunan Province (No. 18B004).

Supplementary materials

Supplementary material associated with this article can be found, in the online version, at doi:10.1016/j.cclet.2021.09.036.

References

[1] Y.F. Kang, L.Y. Niu, Q.Z. Yang, Chin. Chem. Lett. 30 (2019) 1791–1798.
[2] Y. Yue, F. Huo, F. Cheng, et al., Chem. Soc. Rev. 48 (2019) 4155–4177.
[3] L. Yang, H. Xiong, Y. Su, et al., Chin. Chem. Lett. 30 (2019) 563–565.
[4] A.J. Kowaltowski, N.C. de Souza-Pinto, R.F. Castilho, A.E. Vercesi, Free Radical Bio. Med. 47 (2009) 333–343.
[5] E. Bertero, C. Maack, Circ. Res. 122 (2018) 1460–1478.
[6] S. Kausar, F. Wang, H. Cui, Cells 7 (2018) 274.
[7] L. He, Y. Jiang, J. Green, H. Blevins, S. Zhang, Bioorg. Med. Chem. Lett. 29 (2019) 1957–1961.
[8] P. Hernansanz-Agustín, J.A. Enríquez, Antioxidants 10 (2021) 415.
[9] S.S. Liew, X. Qin, J. Zhou, et al., Angew. Chem. Int. Ed. 60 (2021) 2232–2256.
[10] S. Lee, J. Li, X. Zhou, J. Yin, J. Yoon, Coordin. Chem. Rev. 366 (2018) 29–68.
[11] Y. Yue, F. Huo, C. Yin, Chem. Sci. 12 (2021) 1220–1226.
[12] N. Zhou, F. Huo, Y. Yue, K. Ma, C. Yin, Chin. Chem. Lett. 31 (2020) 2970–2974.
[13] H. Zhang, P. Xu, X. Zhang, et al., Chin. Chem. Lett. 31 (2020) 1083–1086.
[14] D. Li, W. Chen, S.H. Liu, X. Chen, J. Yin, Chin. Chem. Lett. 31 (2020) 2891–2896.
[15] L. He, X. Yang, K. Xu, X. Kong, W. Lin, Chem. Sci. 8 (2017) 6257–6265.
[16] M. Sibrian-Vazquez, J.O. Escobedo, S. Lim, G.K. Samoei, R.M. Strongin, Proc. Natl. Acad. Sci. U. S. A. 107 (2010) 551–554.
[17] Y. Huang, Y. Zhang, F. Huo, et al., J. Am. Chem. Soc. 142 (2020) 18706–18714.
[18] J. Liu, Y.Q. Sun, Y. Huo, et al., J. Am. Chem. Soc. 136 (2014) 574–577.
[19] Y. Li, W. Liu, P. Zhang, et al., Biosens. Bioelectron. 90 (2017) 117–124.
[20] Y. Li, W. Liu, H. Zhang, et al., Chem. Asian J. 12 (2017) 2098–2103.
[21] S.V. Mulay, Y. Kim, M. Choi, et al., Anal. Chem. 90 (2018) 2648–2654.
[22] C. Cao, Y. Feng, H. Li, et al., Talanta 219 (2020) 121353.
[23] Z. Xu, T. Qin, X. Zhou, L. Wang, B. Liu, Trends Anal. Chem. 121 (2019) 115672.
[24] S. Yang, C. Guo, Y. Li, et al., ACS Sens. 3 (2018) 2415–2422.
[25] K. Xiong, F. Huo, J. Chao, Y. Zhang, C. Yin, Anal. Chem. 91 (2019) 1472–1478.
[26] G. Yin, Y. Gan, H. Jiang, et al., Anal. Chem. 93 (2021) 9878–9886.
[27] J. Zhang, X. Bao, J. Zhou, et al., Biosens. Bioelectron. 85 (2016) 164–170.
[28] T.B. Ren, Q.L. Zhang, D. Su, et al., Chem. Sci. 9 (2018) 5461–5466.
[29] J. Chen, X. Jiang, C. Zhang, et al., ACS Sens. 2 (2017) 1257–1261.
[30] X. Zhang, Y. Huang, X. Han, et al., Anal. Chem. 91 (2019) 14728–14736.
[31] R. Zhang, J. Yong, J. Yuan, Z. Ping Xu, Coordin. Chem. Rev. 408 (2020) 213182.
[32] P. Gao, W. Pan, N. Li, B. Tang, Chem. Sci. 10 (2019) 6035–6071.
[33] Z. Xu, X. Huang, X. Han, et al., Chem 4 (2018) 1609–1628.
[34] Z. Xu, X. Huang, M.X. Zhang, et al., Anal. Chem. 91 (2019) 11343–11348.
[35] G.x. Yin, T.t. Niu, Y.b. Gan, et al., Angew. Chem. Int. Ed. 57 (2018) 4991–4994.
[36] G. Yin, T. Niu, T. Yu, et al., Angew. Chem. Int. Ed. 58 (2019) 4557–4561.
[37] D.I. Danylchuk, P.H. Jouard, A.S. Klymchenko, J. Am. Chem. Soc. 143 (2021) 912–924.
[38] S. Gong, Z. Zheng, X. Guan, S. Feng, G. Feng, Anal. Chem. 93 (2021) 5700–5708.